



Ebullition dominates high methane emissions globally across all lake sizes

Jonas Stage Sørensen¹ · Kenneth Thorø Martinsen² ·
Theis Kragh¹ · Kaj Sand-Jensen²

Received: 15 October 2024 / Accepted: 9 April 2025
© The Author(s) 2025

Abstract Methane is emitted from lakes by diffusion and ebullition. Methane diffusion is constrained by diffusion from sediments to water and water to the atmosphere, as well as oxidation. Methane ebullition from shallow water sediments bypasses these constraints but requires high methane production to form bubbles. We tested if ebullition dominates at high emissions with a Danish dataset and a global dataset comprising 973 measurements. Upper limits of methane diffusion were more constrained than ebullition. During periods of low total emissions, diffusive methane emissions predominated, whereas ebullition prevailed during periods of high emissions. The relative contribution of ebullition changed predictably, being 50% at 1.5–1.6 mmol m⁻² d⁻¹ and 75% at 5.1–6.4 mmol m⁻² d⁻¹ total methane emission. The probability of ebullitive flux was highly affected by

the magnitude of the diffusive flux, and water temperature. Thus, when data was divided into the water temperature intervals ≤10, 10–20, and >20 °C, ebullition occurred in 69, 69 and 95% of the observations, respectively, and emission increased from 0.29, 0.71 to 3.6 mmol m⁻² d⁻¹ between the three temperature intervals. Summed across all measurements, ebullition accounted for the majority (75–83%) of total methane emissions. Thus, to attain reliable whole-lake emission and global estimates, many ebullition measurements are required to cover their extensive spatial and temporal variability.

Keywords Methane · Ebullitive · Diffusive · Greenhouse gas · Emissions

Introduction

Methane emission from lake surfaces contributes a high percentage to the global emissions compared to overall methane emissions (15–19%), although lake surfaces only cover a small percentage (~ 3%) of the land area (Downing et al. 2006; Johnson et al. 2022; Saunio et al. 2020).

Methane ebullition increases with higher temperatures (Aben et al. 2017), however, even at low water temperatures, ebullition occurs (Sørensen et al. 2024a). Methane production is high and variable in anoxic lake sediments rich in easily degradable organic matter from the catchment and in-lake production

Responsible Editor: J.M. Melack

Supplementary Information The online version contains supplementary material available at <https://doi.org/10.1007/s10533-025-01233-8>.

J. S. Sørensen (✉) · T. Kragh
University of Southern Denmark, Campusvej 55,
5230 Odense M, Denmark
e-mail: jonassoe@biology.sdu.dk

K. T. Martinsen · K. Sand-Jensen
Freshwater Biological Laboratory, Department of Biology,
University of Copenhagen, Universitetsparken 4, 3rd Floor,
2100 Copenhagen, Denmark

(Beaulieu et al. 2019; West et al. 2016). Proper quantification of methane efflux from a large variety of lakes (including ponds and impoundments) is essential for an evaluation of their role as sources of greenhouse gases (GHG) in large-scale carbon budgets (Johnson et al. 2022; Rosentreter et al. 2021).

Methane production in sediment increases as temperature rises, resulting in higher rates during summer than winter in temperate and arctic regions. By contrast, methane production is inhibited by the presence of oxygen or alternative electron acceptors (e.g. nitrate, sulfate, ferric iron) (Fenchel et al. 2012), and methane diffusing from reduced deep sediment layers may be oxidized when exposed to sulfate or oxygen closer to the sediment surface (Frenzel et al. 1990; Iversen & Jørgensen 1985). Methane may also be produced in oxic phytoplankton communities as a by-product of methylphosphonate decomposition, however, the magnitude and importance of this process is not clear (Günthel et al. 2020; Thottathil et al. 2022).

Measurements of methane emissions from lakes are challenging. Methane emission takes place both by diffusion (F_{diff}) from the lake surface and as bubbles (ebullition; F_{ebul}) that are produced and released from the sediment and rise through the water column to the surface. Furthermore, plant-mediated methane emission occurs but is not included in this paper (Bastviken et al. 2023). The diffusive flux is variable in time and space due to changes in methane water concentration (C_{wat}) and gas exchange velocity (k). But methane ebullition is even more variable because methane production is susceptible to the quantity and quality of sediment organic matter (Wik et al. 2013, 2018), and the physical properties of the sediment influence the release of bubbles; i.e. sediment particle size and organic content influence bubble formation and release (DelSontro et al. 2015; West et al. 2016). Coarse, organic-poor sediments never or rarely form bubbles, while organic-rich and muddy sediments often do (Sø et al. 2023b). Bubbles are not released at predictable intervals, but often as bursts followed by pauses of variable duration (DelSontro et al. 2015). New bubbles are formed during pauses until one reaches sufficient size and buoyancy to enable passage through and release from the sediment surface (Schmid et al. 2017; Walter et al. 2007). This bubble may be followed by additional bubbles, likely due to reduced physical resistance mediated by the passage of the first (Sø et al. 2023b).

Here, we report our daily measurements of diffusive and ebullitive fluxes in 568 daily values from Danish lakes and 405 daily values from international lakes compiled from 61 publications covering an extensive range of lake surface area (0.000002–67,075 km²). Our three hypotheses are that: 1. The upper limit for F_{diff} is both lower and more constrained than F_{ebul} from lake surfaces, and 2. As total methane flux (F_{total}) increases, the relative contribution of F_{ebul} increases, and F_{diff} decreases, and 3. the probability of F_{ebul} in a flux measurement increases with water temperature.

Methods and materials

Data

The Danish dataset provides hourly measurements during summer and winter (Sø et al. 2023b) that were combined into 568 daily measurements, including 309 from six very small lakes presented earlier (Sø et al. 2024a), but now expanded with data from larger lakes. Our dataset consisted of ten lakes ranging in size and max depth from 878–130,000 m² and 0.5–12 m, respectively. In the smallest lakes (<10,000 m²), four chambers were deployed for approximately a week; this was done twice during winter and once during summer. Two of the lakes in the dataset was measured for a period of five days at 85 and 37 stations, whereas the remaining two lakes were measured for approximately a week. The stations were distributed to cover a gradient from shallow to deeper sites in each lake.

F_{diff} and F_{ebul} were measured in floating chambers with automatic methane sensors recording concentrations every 2 s for 40 minutes, followed by automatic venting of the headspace volume with new atmospheric air for 20 minutes permitting a new subsequent measurement series (Sø et al. 2024b). Fluxes were calculated for every hour using a running variance method (Sø et al. 2023a, 2024b). The method allows for separation of ebullitive and diffusive fluxes, by distinguishing ebullition events as periods of high running variance. Diffusive fluxes are calculated as a linear increase and only prior to ebullitive events. The method provides visual inspection of all fluxes. For the present study, we integrated 24 hourly fluxes for each chamber position into a daily flux (Sø et al.

2024a, 2023b). The battery supply allowed measurements for over a week with no manual inspection.

The literature dataset includes 405 measurements of F_{diff} or F_{total} in floating chambers, eddy covariance or by Fick's Law and F_{ebul} in separate bubble traps compiled from 53 peer-reviewed publications (See supplementary, Figure S1). In the literature, we searched for studies and datasets reporting F_{ebul} , F_{diff} and/or C_{wat} in lakes. From articles reporting F_{ebul} and F_{diff} emissions, we extracted data on lake surface area, location, and measurement method. Various measurement techniques were used to evaluate F_{ebul} in the literature data, with the most common method being bubble traps (43% of the literature data; see supplementary data) and the second-most (20%) by separation of F_{diff} and F_{ebul} through k_{600} -values, followed by discrete chamber measurements (18%), continuous high frequent measurements (7%), lake-ice surveys (7%) and the remaining (6%) hydroacoustically, optical methane detector or not explained. F_{diff} was measured either through discrete gas chamber measurements (41%), continuous high frequent measurements (31%), boundary layer models (25%) and the remaining as either eddy covariance towers (2%) or not explained (1%). The total flux (F_{total}) was calculated as the sum of F_{ebul} and F_{diff} . When only two variables were reported, their relationship enabled the third one to be calculated. We also determined the contribution of F_{ebul} to F_{total} .

Analysis

To evaluate the constraints on F_{diff} from lake surfaces, we compared observations of F_{diff} and estimates based on bootstrapping simulations using the boundary layer model. We used 390 observations of C_{wat} and 2312 observations (negative values removed) of gas transfer velocity (k_{600} , i.e. k normalized to a Schmidt number of 600 (CO_2 at 20 °C) from Klaus and Vachon (2020) to simulate F_{diff} for five lake area categories ($0\text{--}10^4$, $10^4\text{--}10^5$, $10^5\text{--}10^6$, $10^6\text{--}10^7$ and $> 10^7$ m^2) by randomly selecting 10,000 times with replacement. C_{air} was calculated using Henry's Law (Sander 2015) and an atmospheric partial pressure of 2 ppm. C_{air} and k for methane at 10 °C were determined (F_{diff} is only marginally affected by temperature due to increase in methane oxidation with temperature, see Figure S2).

We used linear models to analyze the relationship between lake surface area and C_{wat} , k and F_{diff} , \log_{10} -transforming both the independent and dependent variables (except for the $F_{\text{ebul}}:F_{\text{total}}$ ratio). The relationship between $F_{\text{ebul}}:F_{\text{total}}$ and lake surface area were assessed using beta-regression because the dependent variable is a ratio. A hyperbolic model was used to analyze the relationship between F_{ebul} to F_{total} according to:

$$F_{\text{ebul}} = \frac{F_{\text{max}} * F_{\text{total}}}{(K_{1/2} + F_{\text{total}})},$$

F_{max} is the upper boundary of the model (0–1), $K_{1/2}$ is F_{total} at $F_{\text{ebul}} = 0.5 * F_{\text{max}}$. The model was fitted to the running median of F_{ebul} over 100 points to reduce noise. To determine the effect of water temperature on the probability of ebullition we used a logistic regression with water temperature and F_{diff} as the independent variables. The F_{diff} was used rather than the F_{total} which is not independent due to it being partly determined by F_{ebul} . Additionally, we analyzed the spread of flux observations using the median and density plots for intervals of water temperature to determine the effect of water temperature on fluxes (≤ 10 °C, 10–20 °C and > 20 °C). Water temperature was extracted from the Danish data and the literature when reported and was available for 851 observations (87%). For the logistic regression both water temperature and F_{diff} were scaled according to mean and standard deviation to be able to compare the results.

Beta-regression was performed using the *betareg* R-package (Zeileis et al. 2016), and the statistical programming software R (R Core Team 2018) was used for all analyses.

Results

F_{diff} and F_{ebul} were left-skewed in the Danish and literature data (Fig. 1 and Table 1). Median fluxes in the 90th and 95th percentiles were 3–5 times lower for F_{diff} than F_{ebul} (Table 1). While the 90th percentile:median was 3.6 and 6.4 for F_{diff} compared with 13.7 and 17.9 for F_{ebul} in the two datasets (Table 1). The distribution of upper thresholds (i.e. from 90th to 95th percentiles) was also narrower, relative to the medians, for the F_{diff} (1.7–4.2) than the F_{ebul} (9.4–10.7, Table 1).

Fig. 1 Frequency distribution of F_{ebul} , F_{diff} and F_{total} methane fluxes from lakes and ponds in Danish and literature measurements. Vertical lines show medians and 90th and 95th percentiles

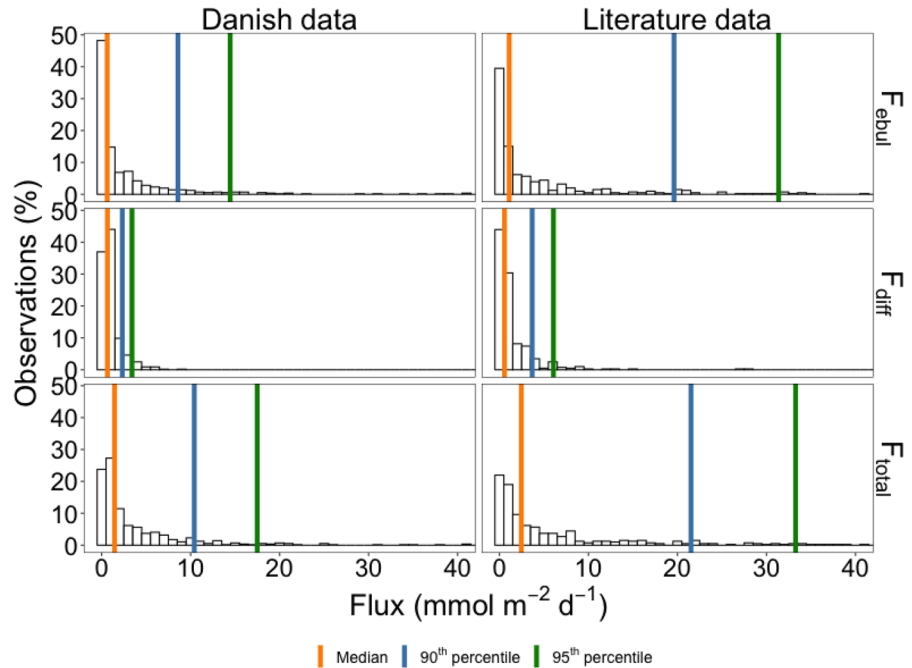


Table 1. Median and 90 and 95 percentile of the distribution of diffusive, ebullitive and total methane fluxes from ponds and lakes in Danish and literature measurements

Flux	Median		90th percentile		95th percentile		90th:median		95th:median		(95th–90th):median	
	Danish	Literature	Danish	Literature	Danish	Literature	Danish	Literature	Danish	Literature	Danish	Literature
F_{diff}	0.65	0.57	2.32	3.68	3.41	6.07	3.58	6.42	5.26	10.59	1.67	4.17
F_{ebul}	0.63	1.10	8.57	19.61	14.44	31.37	13.71	17.85	23.11	28.54	9.39	10.69
F_{total}	1.45	2.46	10.41	21.52	17.48	33.27	7.18	8.75	12.05	13.53	4.88	4.78

Unit: $\text{mmol m}^{-2} \text{d}^{-1}$

Data compiled from the literature on C_{wat} and k are left-skewed, with 80% of C_{wat} below $3 \mu\text{M}$ and 83% of k_{600} values below 2 m d^{-1} (Fig. 2A-B). The frequency distribution of observed and bootstrap-simulated F_{diff} resemble each other for the four smallest lake size categories, with generally lower fluxes for larger lakes (Fig. 2C). Apart from somewhat higher values for a single lake size category (10^4 – 10^5 m^2), the medians of simulated F_{diff} are located within a narrow range (0.18 – $0.91 \text{ mmol m}^{-2} \text{d}^{-1}$; Table 2) resembling the medians of measured F_{diff} (0.57 – $0.65 \text{ mmol m}^{-2} \text{d}^{-1}$; Table 1). Likewise, the 90th and 95th percentiles of simulated F_{diff} for those four size categories were (3.06 – 5.16 and 4.96 – $9.19 \text{ mmol m}^{-2} \text{d}^{-1}$; Table 2), similar

to the upper percentiles for the measured fluxes (2.12 – 4.05 and 3.39 – $6.78 \text{ mmol m}^{-2} \text{d}^{-1}$; Table 1).

C_{wat} decreased linearly with lake surface area (linear model: $\log_{10}(\text{CH}_4) = -0.23 \cdot \log_{10}(\text{area}) + 1.35$, $R^2 = 0.29$, $p < 0.001$; Fig. 3A) while F_{diff} decreased initially and then increased in lakes larger than 10^8 m^2 ($\log_{10}(F_{\text{diff}}) = -1.29 \cdot \log_{10}(\text{area}) + 0.08 \cdot (\log_{10}(\text{area}))^2 + 4.6$, $R^2 = 0.15$, $p < 0.001$; Fig. 3C). The decrease in F_{diff} with increasing lake surface area is also visible in the simulated F_{diff} (Fig. 2C). k_{600} increased initially, with lake size reaching an upper level of 1 m d^{-1} at approximately 10^6 m^2 ($\log_{10}(k_{600}) = 0.62 \cdot \log_{10}(\text{area}) - 0.04 \cdot (\log_{10}(\text{area}))^2 - 2.19$, $R^2 = 0.31$, $p < 0.0001$; Fig. 3B). Despite the inverse relationship between

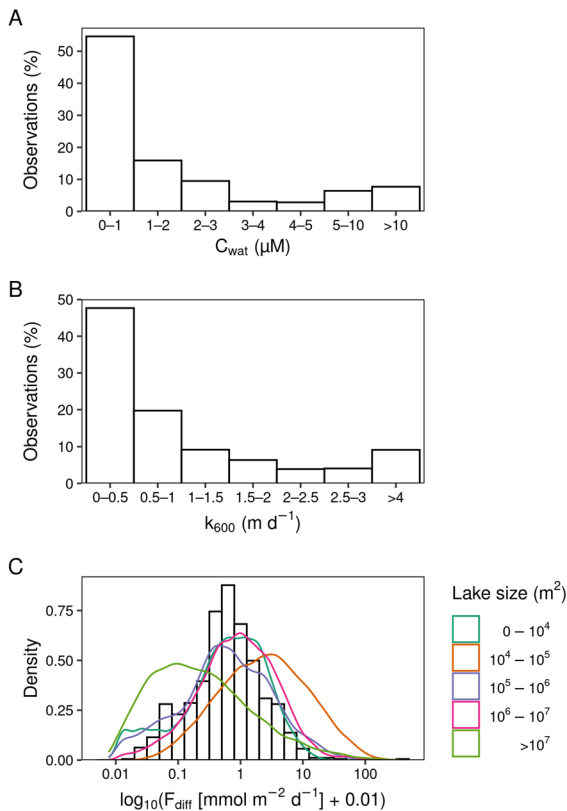


Fig. 2 Frequency distribution of C_{wat} (A), k_{600} (B), and observed F_{diff} (bars) and F_{diff} (lines) simulated by bootstrapping where F_{diff} is determined from random draws of gas transfer velocity and C_{wat} at 10 °C

C_{wat} and k_{600} , small lakes with a surface area of less than 10^5 m^2 appeared to sustain higher F_{diff} .

Measured F_{diff} accounted for most of the F_{total} at low total emissions, while its contribution diminished at high total emissions (Fig. 4). In contrast, the contribution of F_{ebul} to F_{total} was small at low total emissions, while it closely resembled it at high total emissions. Thus, the contribution of F_{ebul} relative to

F_{diff} increased with the magnitude of F_{total} , while the contribution of F_{diff} decreased (Fig. 5). A predictable hyperbolic curve was observed for the Danish data and literature data. Thus, diffusion contributed 75% and ebullition 25% at F_{total} of 0.7–1.0 $\text{mmol m}^{-2} \text{ d}^{-1}$ for both data sets. Equal contribution of F_{diff} and F_{ebul} was found at F_{total} of 1.5–1.6 $\text{mmol m}^{-2} \text{ d}^{-1}$, while F_{ebul} contributed 75% and diffusion 25% to F_{total} of 5.1–6.4 $\text{mmol m}^{-2} \text{ d}^{-1}$. When F_{total} was even higher, the contribution of F_{ebul} approached 100%. Summed across the Danish and literature measurements, ebullition accounted for the great majority (75–83%) of total methane emissions.

In 620 of the observations, ebullition was detected, accounting for 73% of all observations. The logistic regression had a significant positive effect of water temperature and F_{diff} on the probability of ebullition (water temperature: estimate = 0.05, $p < 0.001$; F_{diff} : estimate = 1.6, $p < 0.001$), indicating higher probability of ebullition with higher water temperature and/or F_{diff} . This pattern was also observed between the three water temperature intervals (≤ 10 , 10–20 and > 20 °C) displaying ebullition in 69, 69 and 95% of the observations, respectively. Median F_{diff} showed only little variation with increasing temperature 0.67, 0.57 and 0.73 $\text{mmol m}^{-2} \text{ d}^{-1}$ in the ≤ 10 , 10–20 and > 20 °C intervals, respectively (Fig. 6). However, median F_{ebul} in the same temperature intervals were 0.29, 0.71, and 3.6 $\text{mmol m}^{-2} \text{ d}^{-1}$, respectively (Fig. 6).

Discussion

Bubble formation requires methane production that exceeds the diffusive sediment loss. With increasing depth, higher methane production is required to overcome the additional hydrostatic pressure; in addition, a longer passage to the water surface leads to larger

Table 2. F_{diff} ($\text{mmol m}^{-2} \text{ d}^{-1}$) simulated by bootstrapping where F_{diff} is determined from random draws of gas transfer velocity (k_{600}) and C_{wat} from different lake size classes. Mean k_{600} and C_{wat} of each lake size class are also denoted

Lake area (m^2)	k_{600} (m d^{-1})	C_{wat} (μM)	Median ($\text{mmol m}^{-2} \text{ d}^{-1}$)	90th percentile ($\text{mmol m}^{-2} \text{ d}^{-1}$)	95th percentile ($\text{mmol m}^{-2} \text{ d}^{-1}$)
0– 10^4	0.37	4.93	0.66	3.37	4.96
10^4 – 10^5	1.42	7.08	2.41	20.07	33.88
10^5 – 10^6	1.06	2.55	0.58	4.88	9.19
10^6 – 10^7	2.58	1.22	0.91	5.16	8.14
$>10^7$	1.79	1.66	0.18	3.06	8.06

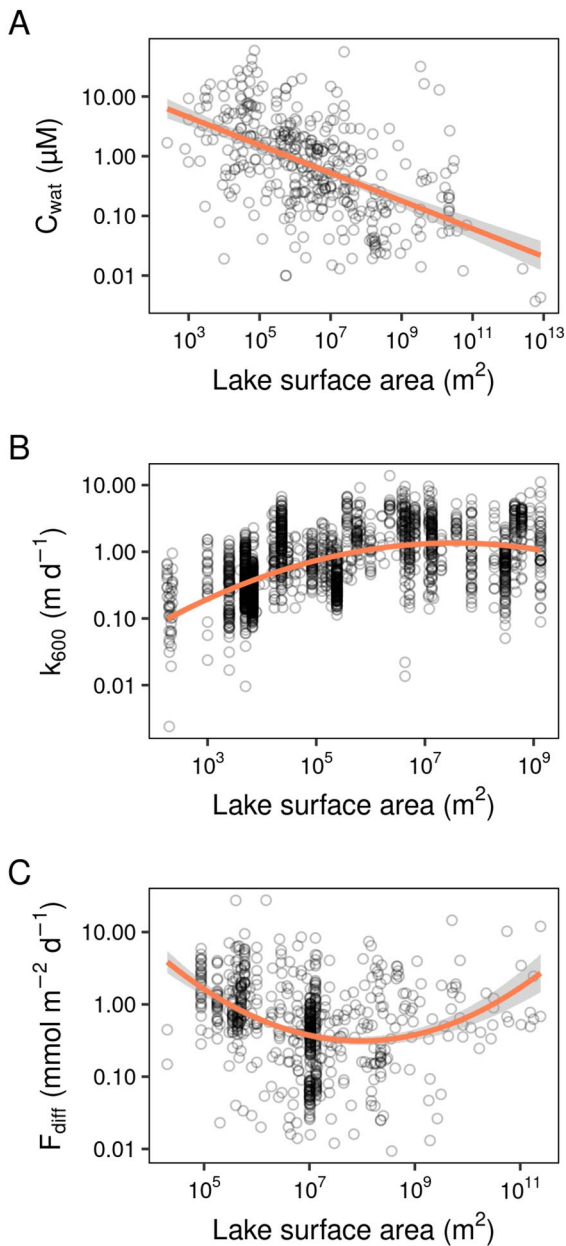


Fig. 3 C_{wat} (A), k_{600} (B), and F_{diff} (C) as a function of lake surface area from 390, 2312, and 732 observations, respectively, compiled from the literature. Solid lines show relationships and grey areas are 95% CIs

methane losses from ascending bubbles (Ostrovsky et al. 2008; West et al. 2016). In the shallow lakes (max depth 1–12 m) from which we collected data, water depth is not expected to cause bubble dissolution and thus not change the balance between F_{diff}

and F_{ebul} to the atmosphere, but F_{ebul} likely declines at greater water depths (> 20 m) due to dissolution of the ascending bubbles (Schmid et al. 2017).

The Danish and compiled literature data both showed a higher constrain on the 95th percentiles of F_{diff} , being 4–5-fold lower than F_{ebul} , which accords with our first hypothesis. Relative to median levels, the 90th and 95th percentiles were much lower for F_{diff} than F_{ebul} , and the range between the 90th and 95th percentiles was narrower for F_{diff} than F_{ebul} . Thus, F_{ebul} attained much higher and more variable rates than F_{diff} .

Methane produced in sediment does not accumulate and form bubbles until production surpasses diffusive losses to the bottom waters. F_{ebul} as a proportion of F_{total} rose hyperbolically with increasing F_{total} , due to the physical constraints on F_{diff} within sediment and water–air release (Bazhin 2003), but not on bubble release from sediment, as proposed in our second hypothesis. In both datasets, when F_{total} was approximately 1.5–1.6 $\text{mmol m}^{-2} \text{d}^{-1}$, F_{diff} and F_{ebul} were close to 1:1, but above this level, ebullition took over and comprised 75% of F_{total} at 5.1–6.4 $\text{mmol m}^{-2} \text{d}^{-1}$. In early global budgets of methane release from lakes at all latitudes, F_{ebul} were responsible for the main (77–90%) of F_{total} (Bastviken et al. 2011). In the comprehensive compilation of Danish and literature data summed across all measurements, F_{ebul} accounted for the main percentage (75–83%) of F_{total} .

Large lake size increases wind exposure and fetch, which facilitates greater gas exchange velocity (Vachon & Prairie 2013) (Fig. 3B) and possibly also facilitates diffusive methane release from sediments, provided the diffusive boundary layer becomes thinner (Jørgensen & Revsbech 1985). This is particularly important in shallow lakes and less so in deeper lakes. In contrast, recent research has shown that k is affected by multiple parameters besides wind, such as differential heating or cooling and atmospheric stability, resulting in an underestimation of k in low wind systems such as smaller lakes and thereby underestimating fluxes (MacIntyre et al. 2021a, 2021b).

The hyperbolic relationship describing the ratio between F_{ebul} and F_{total} is fitted for the large dataset of shallow lakes we examined as well as for the literature data of global lakes and the restricted data for ponds examined earlier (Sø et al. 2024a). Thus, this pattern is probably representative of the majority of standing freshwaters worldwide (Sø et al. 2024a), and

Fig. 4 The relative contribution of F_{ebul} to F_{total} in Danish and literature data. The line shows the running median of 100 points, while the shaded area indicates the running 25th–75th percentiles of 100 points. Orange line indicates the hyperbolic relationship. F_{max} was 1 for both of the models, whereas $K_{1/2}$ was 2.2 and 1.9 for the Danish and literature data, respectively

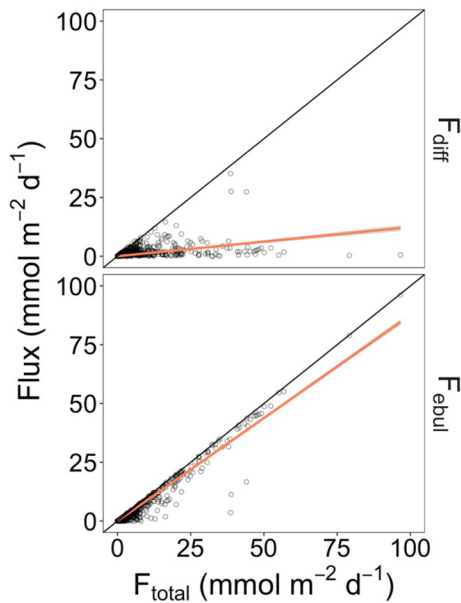
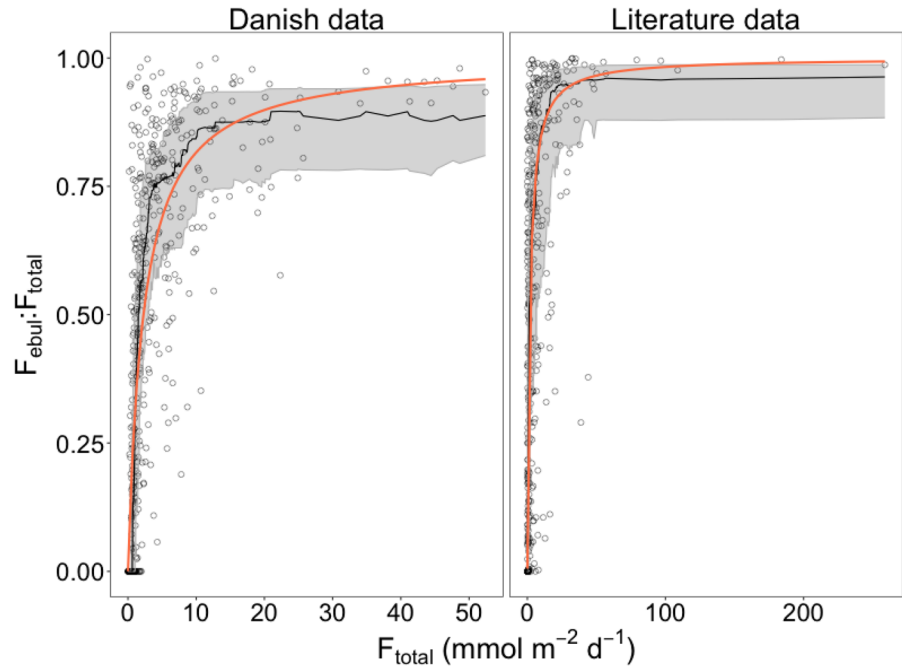


Fig. 5 F_{diff} and F_{ebul} in relation to F_{total} in upper and lower panels, respectively. The regression line of F_{diff} to F_{total} was: $F_{\text{diff}} = 0.12 * F_{\text{total}}$ (t-value 18.6, $p < 0.001$) and the regression line of F_{ebul} to F_{total} was: $F_{\text{ebul}} = 0.88 * F_{\text{total}}$ (t-value 131.7, $p < 0.001$). The black line shows the 1:1 line. Three points above $100 \text{ mmol m}^{-2} \text{ d}^{-1}$ with F_{ebul} very close to F_{total} were omitted for clarity

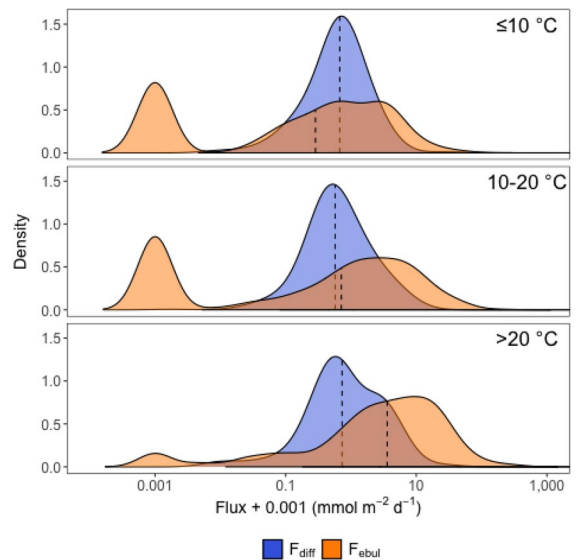


Fig. 6 Density plots of F_{diff} and F_{ebul} at three different temperature intervals ($\leq 10 \text{ }^\circ\text{C}$, $10\text{--}20 \text{ }^\circ\text{C}$ and $> 20 \text{ }^\circ\text{C}$). Dashed lines indicate median values. 0.001 was added to all fluxes to include 0-values in logarithmic axis

probably universal for all lakes, regardless of size. For example, ebullitive fluxes dominate diffusive emissions in medium-sized, relatively deep (mean depth 26 m) Lake Kinneret (Schmid et al. 2017). However,

in large deep lakes (> 50 m, mean depth), the higher methane partial pressure required to overcome hydrostatic pressure and form bubbles, and more methane dissolution (> 80–90%) from ascending bubbles as they travel to the water surface (DelSontro et al. 2016; Ostrovsky et al. 2008; West et al. 2016) preclude ebullitive emission and constrain methane losses to the atmosphere overall. In such large deep lakes, F_{ebul} may be restricted to the shallow littoral zone, which covers only a very small proportion of their surface (Bastviken et al. 2004; Linkhorst et al. 2020).

We tested the firm constraints on the maximum F_{diff} from lake surfaces by simulating F_{diff} , using C_{wat} and k for various lake size classes, based on available literature data. The 90th and 95th percentiles resembled those attained in floating chamber measurements in shallow lakes. Despite the inverse relationship between decreasing C_{wat} and increasing k with increasing lake surface area, simulated F_{diff} was generally higher in small than medium-sized lakes. Although F_{diff} did increase in large lakes (> 10^8 m^2) this response is based on relatively few measurements. Thus, the results supports an inverse relationship between C_{wat} and k tending to stabilize F_{diff} across lake sizes. The probability that ebullition occurred was positively affected by water temperature and F_{diff} , with the effect of F_{diff} being more than 8 times higher than water temperature. However, this data only shows that ebullition was present during the day and not how many bubbles were released. In the three water temperature intervals (≤ 10 , 10–20, and > 20 °C), only little difference in median F_{diff} was observed, and no clear pattern towards elevated fluxes in the higher temperature intervals. In contrast, median F_{ebul} increased more than 10-fold across the three temperature intervals. Clearly, F_{ebul} markedly increased in magnitude in warmer water and ebullition was almost always present above 20 °C, most likely caused by an increase in the number of bubbles rather than their size. It is worth noticing that even at low water temperature, ebullition still occurs, which has also previously been shown (Sø et al. 2024a; Walter Anthony et al. 2010). F_{diff} did not experience a similar increase with increasing water temperature but remained stable between intervals. Higher water temperature would increase methane production (Schulz et al. 1997), but despite large water temperature differences, we did not observe changes in median F_{diff} between temperature intervals. Clearly, much more

methane is lost through ebullition, whereas the lack of higher F_{diff} could be caused by increasing methane oxidation with temperature in the water keeping methane concentrations and diffusive loss unaltered (Thottathil et al. 2019).

Our results agree with previous results showing an increased F_{ebul} with water temperature (Aben et al. 2017; DelSontro et al. 2016). Moreover, we show that the probability of ebullition and, in particular, the magnitude and contribution of F_{ebul} to F_{total} increase extensively above 20 °C in accordance with hypothesis 3.

Based on our results, we stress that *in situ* measurements are required to quantify both F_{diff} and F_{ebul} from lake surfaces. Ebullition is particularly variable in time and space, and many measurements at high temporal and spatial resolution are needed to attain a reliable whole-lake value (Sø et al. 2023b; Wik et al. 2016). When methane emission is intense, at high summer temperatures (Sø et al. 2024a), the contribution of F_{ebul} approaches or exceeds 90% of F_{total} (Fig. 4) and a fine grid of measurements becomes essential.

Floating chambers equipped with do-it-yourself electronics and inexpensive sensors, as introduced by Bastviken et al. (2020) and modified and improved by Sø et al. (2023b), can be deployed in large numbers to ensure the required spatial resolution and, moreover, provide simultaneous hourly measurements of F_{ebul} , F_{diff} and, thus, F_{total} . Other available methods do not offer these advantages. Laser equipment offers sensitive measurements at high temporal resolution but is expensive, and laser sensors cannot be inserted in many chambers and provide high spatial resolution, whereas the large measurement footprint of eddy covariance systems can make it difficult to quantify emissions and drivers of small-scale emissions hotspots. A high spatial resolution of ebullition can be attained by using sonar equipment to assess the rate and size distribution of bubble release, in which measurements of bubble methane content must assist (DelSontro et al. 2015; Ostrovsky et al. 2008). All of the above methods and more were used in the literature data when determining the F_{ebul} , thereby introducing a possibility for variation and uncertainty of the data. However, to our knowledge, no studies have been done to assess the variation in results from different methods when measuring F_{ebul} and we were

left to accept the validity of the published data when methods and calculations were carefully explained.

Despite the advantages of floating chambers to provide fluxes of CH₄ and CO₂ at high spatial and temporal resolution, the workload remains substantial in all local approaches, so, to upscale measurements from individual lakes and attain integrated national and global budgets; we recommend searching for general predictions of reliable whole-lake methane fluxes as a function of important lake characteristics across geographic location, morphometry, trophic state, and vegetation cover.

Author contributions The project was conceptualized with input from all authors, with Kaj Sand-Jensen (KSJ) being the originator of the idea. Equipment for the Danish measurements was developed by Jonas Stage Sø (JSS) and Theis Kragh (TK) and sampled by JSS and Kenneth Thorø Martinsen (KTM). Literature data was collected and verified by JSS. Analysis and visualization were done by KTM and JSS. Writing the original draft was done by JSS and KSJ, while reviewing and editing was done by all authors.

Funding Open access funding provided by University of Southern Denmark. We thank Aage V. Jensens Nature Foundation for supporting TK and the PhD work of JSS. We thank The Independent Research Fund Denmark for supporting the project "Supporting climate and biodiversity by rewetting low-lying areas" to KSJ (0217-00112B).

Data availability Background theory and data are publicly available from an online repository and can be found here <https://doi.org/https://doi.org/10.5281/zenodo.14942929> (Sø et al. 2025).

Declarations

Conflict of interest The authors declare that they have no known competing financial interests or personal relationships that could have appeared to influence the work reported in this paper.

Open Access This article is licensed under a Creative Commons Attribution 4.0 International License, which permits use, sharing, adaptation, distribution and reproduction in any medium or format, as long as you give appropriate credit to the original author(s) and the source, provide a link to the Creative Commons licence, and indicate if changes were made. The images or other third party material in this article are included in the article's Creative Commons licence, unless indicated otherwise in a credit line to the material. If material is not included in the article's Creative Commons licence and your intended use is not permitted by statutory regulation or exceeds the permitted use, you will need to obtain permission directly from the copyright holder. To view a copy of this licence, visit <http://creativecommons.org/licenses/by/4.0/>.

Reference

- Aben RCH, Barros N, van Donk E, Frenken T, Hilt S, Kazanjian G, Lamers LPM, Peeters ETHM, Roelofs JGM, de Senerpont Domis LN, Stephan S, Velthuis M, Van de Waal DB, Wik M, Thornton BF, Wilkinson J, DelSontro T, Kosten S (2017) Cross continental increase in methane ebullition under climate change. *Nat Commun* 8(1):1682. <https://doi.org/10.1038/s41467-017-01535-y>
- Bastviken D, Cole J, Pace M, Tranvik L (2004) Methane emissions from lakes: Dependence of lake characteristics, two regional assessments, and a global estimate. *Global Biogeochem Cycles*. <https://doi.org/10.1029/2004gb002238>
- Bastviken D, Tranvik LJ, Downing JA, Crill PM, Enrich-Prast A (2011) Freshwater methane emissions offset the continental carbon sink. *Science* 331(6013):50–50
- Bastviken D, Nygren J, Schenk J, Parellada Massana R, Duc NT (2020) Technical note: Facilitating the use of low-cost methane (CH₄) sensors in flux chambers—calibration, data processing, and an open-source make-it-yourself logger. *Biogeosciences* 17(13):3659–3667. <https://doi.org/10.5194/bg-17-3659-2020>
- Bastviken D, Treat CC, Pangala SR, Gauci V, Enrich-Prast A, Karlson M, Gålfalk M, Romano MB, Sawakuchi HO (2023) The importance of plants for methane emission at the ecosystem scale. *Aqua Bot* 184:103596. <https://doi.org/10.1016/j.aquabot.2022.103596>
- Bazhin NM (2003) Theoretical consideration of methane emission from sediments. *Chemosphere* 50(2):191–200. [https://doi.org/10.1016/S0045-6535\(02\)00479-4](https://doi.org/10.1016/S0045-6535(02)00479-4)
- Beaulieu JJ, DelSontro T, Downing JA (2019) Eutrophication will increase methane emissions from lakes and impoundments during the 21st century. *Nat Commun* 10(1):1375. <https://doi.org/10.1038/s41467-019-09100-5>
- DelSontro T, McGinnis DF, Wehrli B, Ostrovsky I (2015) Size does matter: Importance of large bubbles and small-scale hot spots for methane transport. *Environ Sci Technol* 49(3):1268–1276
- DelSontro T, Boutet L, St-Pierre A, del Giorgio PA, Prairie YT (2016) Methane ebullition and diffusion from northern ponds and lakes regulated by the interaction between temperature and system productivity. *Limnol Oceanography* 61(S1):S62–S77
- Downing JA, Prairie Y, Cole J, Duarte C, Tranvik L, Striegl RG, McDowell W, Kortelainen P, Caraco N, Melack J (2006) The global abundance and size distribution of lakes, ponds, and impoundments. *Limnol Oceanography* 51(5):2388–2397
- Fenchel T, Blackburn H, King GM, Blackburn TH (2012) *Bacterial biogeochemistry: the ecophysiology of mineral cycling*. Academic press, USA
- Frenzel P, Thebrath B, Conrad R (1990) Oxidation of methane in the oxic surface layer of a deep lake sediment (Lake Constance). *FEMS Microbiol Ecol* 6(2):149–158
- Günthel M, Klawonn I, Woodhouse J, Bižić M, Ionescu D, Ganzert L, Kümmel S, Nijenhuis I, Zoccarato L, Grossart HP (2020) Photosynthesis-driven methane production in oxic lake water as an important contributor to methane emission. *Limnol Oceanography* 65(12):2853–2865

- Iversen N, Jørgensen BB (1985) Anaerobic methane oxidation rates at the sulfate-methane transition in marine sediments from Kattekat and Skagerrak (Denmark) 1. *Limnol Oceanography* 30(5):944–955
- Johnson, M. S., Matthews, E., Du, J., Genovese, V., & Bastviken, D. (2022). Methane emission from global lakes: new spatiotemporal data and observation-driven modeling of methane dynamics indicates lower emissions. *JGR Biogeosciences*, 127(7), e2022JG006793.
- Jørgensen BB, Revsbech NP (1985) Diffusive boundary layers and the oxygen uptake of sediments and detritus. *Limnol Oceanography* 30(1):111–122
- Klaus M, Vachon D (2020) Challenges of predicting gas transfer velocity from wind measurements over global lakes. *Aquat Sci* 82(3):53. <https://doi.org/10.1007/s00027-020-00729-9>
- Linkhorst A, Hiller C, DelSontro T, Azevedo M, G., Barros, N., Mendonça, R., & Sobek, S. (2020) Comparing methane ebullition variability across space and time in a Brazilian reservoir. *Limnol Oceanography* 65(7):1623–1634. <https://doi.org/10.1002/lno.11410>
- MacIntyre S, Amaral JHF, Melack JM (2021a) Enhanced turbulence in the upper mixed layer under light winds and heating: implications for gas fluxes. *JGR Oceans*. <https://doi.org/10.1029/2020JC017026>
- MacIntyre S, Bastviken D, Arneborg L, Crowe AT, Karlsson J, Andersson A, Gållfalk M, Rutgerström A, Podgrajsek E, Melack JM (2021b) Turbulence in a small boreal lake: Consequences for air–water gas exchange. *Limnol Oceanography* 66(3):827–854. <https://doi.org/10.1002/lno.11645>
- Ostrovsky I, McGinnis DF, Lapidus L, Eckert W (2008) Quantifying gas ebullition with echosounder: The role of methane transport by bubbles in a medium-sized lake. *Limnol Oceanography* 6(2):105–118
- R Core Team. (2018). R: A language and environment for statistical computing. Retrieved from <https://www.R-project.org/>.
- Rosentreter JA, Borges AV, Deemer BR, Holgerson MA, Liu S, Song C, Melack J, Raymond PA, Duarte CM, Allen GH, Olefeldt D, Poulter B, Battin TL, Eyre BD (2021) Half of global methane emissions come from highly variable aquatic ecosystem sources. *Nat Geosci* 14(4):225–230. <https://doi.org/10.1038/s41561-021-00715-2>
- Sander R (2015) Compilation of Henry’s law constants (version 4.0) for water as solvent. *Atmos Chem Phys* 15(8):4399–4981. <https://doi.org/10.5194/acp-15-4399-2015>
- Saunois M, Stavert AR, Poulter B, Bousquet P, Canadell JG, Jackson RB, Raymond PA, Dlugokencky EJ, Houweling S, Patra PK, Ciais P, Arora VK, Bastviken D, Bergamaschi P, Blake DR, Brailsford G, Bruhwiler L, Carlson KM, Carrol M, Castaldi S, Chandra N, Crevoisier C, Crill PM, Covey K, Curry CL, Etiope G, Frankenberg C, Gedney N, Hegglin MI, Höglund-Isaksson L, Hugelius G, Ishizawa M, Ito A, Janssens-Maenhout G, Jensen KM, Joos F, Kleinen T, Krummel PB, Langenfelds RL, Laruelle GG, Liu L, Machida T, Maksyutov S, McDonald KC, McNorton J, Miller PA, Melton JR, Morino I, Müller J, Murguía-Flores F, Naik V, Niwa Y, Noce S, O’Doherty S, Parker RJ, Peng C, Peng S, Peters GP, Prigent C, Prinn R, Ramonet M, Regnier P, Riley WJ, Rosentreter JA, Segers A, Simpson IJ, Shi H, Smith SJ, Steele LP, Thornton BF, Tian H, Tohjima Y, Tubiello FN, Tsuruta A, Viovy N, Voulgarakis A, Weber TS, van Weele M, van der Werf GR, Weiss RF, Worthy D, Wunch D, Yin Y, Yoshida Y, Zhang W, Zhang Z, Zhao Y, Zheng B, Zhu Q, Zhu Q, Zhuang Q (2020) The global methane budget 2000–2017. *Earth System Sci Data* 12(3):1561–1623. <https://doi.org/10.5194/essd-12-1561-2020>
- Schmid M, Ostrovsky I, McGinnis DF (2017) Role of gas ebullition in the methane budget of a deep subtropical lake: what can we learn from process-based modeling? *Limnol Oceanography* 62(6):2674–2698
- Schulz S, Matsuyama H, Conrad R (1997) Temperature dependence of methane production from different precursors in a profundal sediment (Lake Constance). *FEMS Microbiol Ecol* 22(3):207–213
- Sø JS, Sand-Jensen K, Martinsen KT, Polauke E, Kjær JE, Reitzel K, Kragh T (2023b) Methane and carbon dioxide fluxes at high spatiotemporal resolution from a small temperate lake. *Sci Total Environ* 878:162895. <https://doi.org/10.1016/j.scitotenv.2023.162895>
- Sø JS, Martinsen KT, Kragh T, Sand-Jensen K (2024a) Hourly methane and carbon dioxide fluxes from temperate ponds. *Biogeochemistry*. <https://doi.org/10.1007/s10533-024-01124-4>
- Sø JS, Sand-Jensen K, Kragh T (2024b) Self-made equipment for automatic methane diffusion and ebullition measurements from aquatic environments. *JGR Biogeosciences*. <https://doi.org/10.1029/2024JG008035>
- Sø, J. S., Sand-Jensen, K., & Kragh, T. (2023a). FluxSeparator [Software] (Version v1.0.0). Retrieved from <https://zenodo.org/badge/latestdoi/629085131>.
- Sø, J. S., Martinsen, K. T., Kragh, T., & Sand-Jensen, K. (2025). *Ebullition dominates high methane emissions globally across all lake sizes*.
- Thottathil SD, Reis PCJ, Prairie YT (2019) Methane oxidation kinetics in northern freshwater lakes. *Biogeochemistry* 143(1):105–116. <https://doi.org/10.1007/s10533-019-00552-x>
- Thottathil SD, Reis PCJ, Prairie YT (2022) Magnitude and drivers of oxic methane production in small temperate lakes. *Environ Sci Technol* 56(15):11041–11050. <https://doi.org/10.1021/acs.est.2c01730>
- Vachon D, Prairie YT (2013) The ecosystem size and shape dependence of gas transfer velocity versus wind speed relationships in lakes. *Can J Fish Aquat Sci* 70(12):1757–1764
- Walter KM, Smith LC, Stuart Chapin III, F. (2007) Methane bubbling from northern lakes: present and future contributions to the global methane budget. *Phil Trans R Soc A* 365(1856):1657–1676
- Walter Anthony KM, Vas DA, Brosius L, Chapin FS III, Zimov SA, Zhuang Q (2010) Estimating methane emissions from northern lakes using ice-bubble surveys. *Limnol Oceanography* 8(11):592–609
- West WE, Creamer KP, Jones SE (2016) Productivity and depth regulate lake contributions to atmospheric methane. *Limnol Oceanography* 61(S1):S51–S61
- Wik M, Crill PM, Varner RK, Bastviken D (2013) Multi-year measurements of ebullitive methane flux from three

- subarctic lakes. *J Geophys Res: Biogeosci* 118(3):1307–1321. <https://doi.org/10.1002/jgrg.20103>
- Wik M, Thornton BF, Bastviken D, Uhlbäck J, Crill PM (2016) Biased sampling of methane release from northern lakes: A problem for extrapolation. *Geophys Res Lett* 43(3):1256–1262
- Wik M, Johnson JE, Crill PM, DeStasio JP, Erickson L, Halloran MJ, Fahnestock MF, Crawford MK, Phillips SC, Varner RK (2018) Sediment characteristics and methane ebullition in three subarctic lakes. *J Geophys Res Biogeosci* 123(8):2399–2411
- Zeileis, A., Cribari-Neto, F., Gruen, B., Kosmidis, I., Simas, A. B., Rocha, A. V., & Zeileis, M. A. (2016). Package ‘betareg’. *R package*, 3(2).

Publisher’s Note Springer Nature remains neutral with regard to jurisdictional claims in published maps and institutional affiliations.